AD-A178 221 HIGH FREQUENCY FORWARD ACOUSTIC VOLUME SCATTERING AND ITS RELATION TO OCE..(U) IRACOR APPLIED SCIENCES INC SAN DIEGO CA D V HOLLIDAY ET AL. 30 JAN 87 1/1

UNCLASSIFIED IRACOR-I-87-06-7002-U N00014-85-C-0762 F/G 20/1 NL

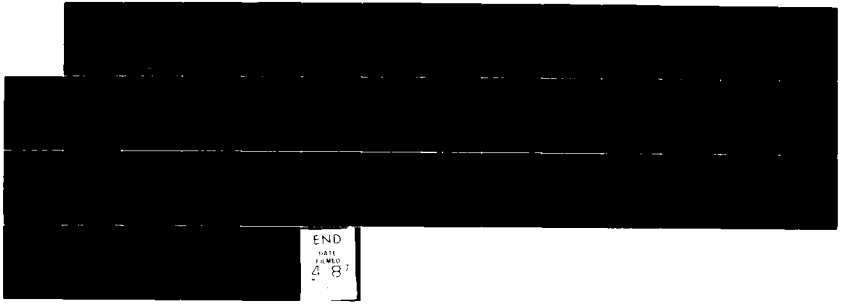

END
DATE FILMED
4 87

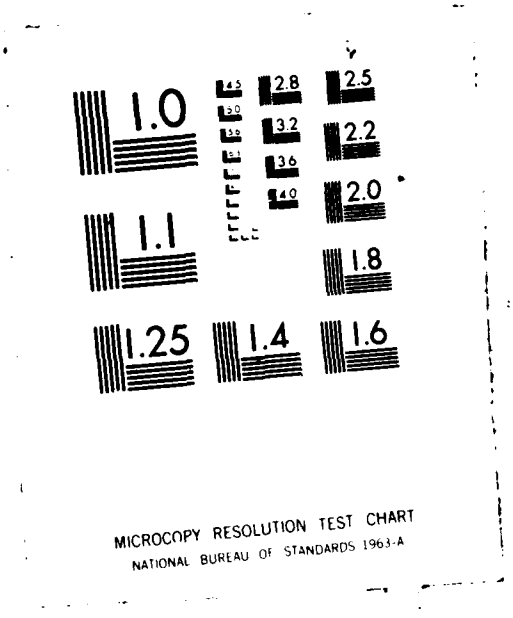
1.0
1.1
1.25
1.4
1.6
1.8
2.0
2.2
2.5
2.8
3.2
3.6
4.0
4.5
5.0
5.6
MICROCOPY RESOLUTION TEST CHART
NATIONAL BUREAU OF STANDARDS 1963-A

Tracor Document No. T-87-06-7002-U
Tracor Project No. 034-023
Contract No. N00014-85-C-0762

FINAL REPORT

on

HIGH FREQUENCY FORWARD ACOUSTIC VOLUME SCATTERING AND ITS RELATION TO OCEANIC FINE STRUCTURE

Submitted to

Commander
Office of Naval Research
801 North Quincy Street
Arlington, VA 22217

Attn: R. Fitzgerald, Code 425UA

A Joint Project of

D. V. Holliday
Tracor Applied Sciences

J. J. McCoy
Statcon

M. J. Beran
Statcon

A. W. Bratkovich
University of Southern California

W. T. Reader
DTNSRDC

January 30, 1987

Tracor Applied Sciences

Tracor Inc. 9150 Chesapeake Drive San Diego, California 92123

Tracor Applied Sciences

Tracor Document No. T-87-06-7002-U
Tracor Project No. 034-023
Contract No. N00014-85-C-0762

FINAL REPORT

on

HIGH FREQUENCY FORWARD ACOUSTIC VOLUME SCATTERING AND ITS RELATION TO OCEANIC FINE STRUCTURE

Submitted to

Commander
Office of Naval Research
801 North Quincy Street
Arlington, VA 22217

Attn: R. Fitzgerald, Code 425UA

A Joint Project of

D.V. Holliday
Tracor Applied Sciences

J.J. McCoy
Statcon

M.J. Beran
Statcon

A.W. Bratkovich
University of Southern California

W.T. Reader
DTNSRDC

January 30, 1987

Preface

This report is the result of a cooperative research program involving five co-principal investigators. The theoretical developments were principally contributed by Mark Beran (Statcon and Tel Aviv University) and John McCoy (Statcon and Catholic University). Van Holliday (Tracor Applied Sciences) carried out the laboratory experiments and served as the project coordinator. Alan Bratkovich (University of Southern California) advised in the aspects of the project that dealt with physical oceanography. Wayne Reader (DTNSRDC) served as an unfunded advisor regarding the effects of acoustic fluctuations on signals of specific interest to the Navy and also offered his experience in dealing with those problems in ocean acoustic measurement programs.

We would like to acknowledge the invaluable assistance of Charles Lee and Mark Niknam in the development of the electronics for the experimental part of the project. Their extra efforts are greatly appreciated. Peter Mull and Tom Boatright also provided valuable help in various phases of the project.

Table of Contents

Table of Contents (con't)

I. Introduction

The long term objectives of this research are to provide a tool for observing oceanic events on a length scale smaller than those associated with internal waves and to provide improved predictive capabilities for direct path propagation fluctuations in the 20 to 70 KHz regime, where small scale events can dominate forward acoustic scattering.

Scattering of an acoustic signal by the dynamic processes and the heterogeneous chemical and physical distribution of properties that exist in the open ocean have received considerable attention in the last decade. Our understanding of the effects of stochastic volume scatter mechanisms on a propagating acoustic field, both at the level of the second-order statistics (signal coherence measures, spread functions) and at the level of fourth-order statistics (signal intensity fluctuations and correlations) is reasonably complete. A comparably detailed description of the structure and mechanisms of physical oceanography at intermediate-to-fine scales is not yet well developed.

This report represents a part of an effort to develop theory on which to base the development of new techniques to be used in developing a better understanding of the intermediate and fine scale physical processes. These are the processes that exist between the spatial scales of internal waves and the dissipative range of turbulent ocean structure. The development of a new technique or tool to study such processes and distributions of ocean properties must include the validation of the mathematical theory on which the technique is to be based. Consequently, some initial efforts directed toward the development of the procedures which are necessary to accomplish that validation are also described in this report.

The obective of this research is to provide a tool that has applicability in many ocean environments. As one attempts to develop a new tool, it is often advantageous to seek out an environment that initially maximizes one's signal and minimizes the measurement noise. That environment should, however, be representative of the ocean. Internal waves often dominate the energy spectrum of processes that influence fluctuations in sound propagation in the temperate oceans. This can make it difficult to separate internal wave induced fluctuations from those caused by simple stochastic heterogeneity in sound speed. The motions of even a relatively large research ship in normal seas would increase the difficulties one might expect to encounter in the accurate measurement of both the acoustic fluctuations and the oceanographic structure.

We have suggested the Arctic as a possible location in which such a technique as is proposed could be tested and developed. The Arctic has the advantage that the internal wave energy appears to be lower than in ice free waters. The technical advantage of making the measurements from a stable platform (the ice) is considered to outweigh the logistical difficulties of working in the Arctic environment. This suggestion is also influenced by a lack of knowledge in the Arctic about the parameters that we would be measuring. Thus, if the Arctic were used as a natural laboratory for a part of the proposed development, there would be an added

advantage of potentially gaining direct, new knowledge about the physical and acoustical oceanography of this unique environment.

In simple terms, our approach is to develop those stochastic models and computer codes that describe the forward scattering process. Those models will involve the parameters of physical oceanography that we ultimately wish to measure. The validation of the models requires measurement of acoustic intensity after it propagates through a medium with a sound speed heterogeneity. It also requires a direct measurement of the stochastic descriptors of the sound speed field. After the validation of the "forward" model, the next step is the solution of the "inverse" problem, i.e., expression of the values for the parameters of physical oceanography in terms of the acoustic measurements. Finally, this "inverse" solution must be successfully compared to experimental measurements.

The frequency or frequencies of the sound used in any tool developed to study the physical oceanography of the ocean must be carefully selected to be optimally sensitive to those phenomena under investigation. As described later in this report, for our application, those frequencies are in the hundreds of kHz to the low MHz range. Ultimately, however, if the proposed tool is successful in developing an accurate description of the basic distribution of ocean properties, one would wish to use the results for predictive purposes. Consequently, the final test we would envision, would be the measurement of forward scattering at frequencies in the 20-70 KHz range and comparison of those measured results with the propagation fluctuations predicted from an estimation of the ocean properties made with the proposed tool (operating at the higher frequencies). This would complete the long range program that we have envisioned.

As an initial effort toward the attainment of the long term goals outlined above, we have conducted a number of theoretical and experimental studies during the term of this contract. These studies have included the following topics. Several additional topics have been covered in an interim report.

1. Extension of the isotropic theory to include anisotropic effects.
2. An assessment of the Arctic as a potential natural laboratory for the testing of the theory.
3. An assessment of the effect of random velocity fluctuations on underwater acoustic scattering.
4. Determination of the intensity distribution from a circular source in an isotropic random medium.
5. A study of the optimum parameters for a laboratory tank experiment.
6. A brief description of the tank experiment.
7. An analysis of results of the tank experiment.

II. Extension of the Isotropic Theory to Include Anisotropic Effects

During the course of this project, the inverse theory for isotropic scattering was extended to include anisotropic effects. We first derived the relevant equations and direct solutions and then found expressions for the inverse relations. Computer codes were written for the solutions in the case of an exponential correlation function. In the case of strong scattering, a simple analytic solution for the Gaussian beam was developed. In addition to considering the measurement of the intensity distribution associated with transmission of a Gaussian sound beam, we also considered measurement of the coherence functions which result from a point source. A computer code was written, and an analytic solution developed, for the case of an exponential correlation function for strong scattering. We also provide analytic expressions for the case of other wave-number power spectra when the scattering is strong.

A. Definitions

To treat the problem from a stochastic point of view we define the following coherence functions:

$$\{\Gamma(\mathbf{x}_{T1},\mathbf{x}_{T2},z)\} = \{u(\mathbf{x}_{T1},z)u^*(\mathbf{x}_{T2},z)\},$$

$$\{L^1(\mathbf{x}_{T1},\mathbf{x}_{T2},\mathbf{x}_{T3},\mathbf{x}_{T4},z)\} =$$

$$\{u(\mathbf{x}_{T1},z)u^*(\mathbf{x}_{T2},z)u^*(\mathbf{x}_{T3},z)u(\mathbf{x}_{T4},z)\}.$$

Here, u^* denotes the complex conjugate of the acoustic field u, and the transverse vector $\mathbf{x}_T$ has the components x and y. The brackets, { }, denote an ensemble average.

The intensity, $\{I(\mathbf{x}_T,z)\}$, is found from $\{\Gamma(\mathbf{x}_{T1},\mathbf{x}_{T2},z)\}$ by setting $\mathbf{x}_{T1} = \mathbf{x}_{T2}$. The intensity fluctuations $\{I^2(\mathbf{x}_T,z)\}$ and the coherence of intensities $\{R_I(\mathbf{x}_{T1},\mathbf{x}_{T2},z)\}$ are found from $\{L^1\}$ from using the following relations:

$$\{I^2(\mathbf{x}_T,z)\} = \{L^1(\mathbf{x}_T,\mathbf{x}_T,\mathbf{x}_T,\mathbf{x}_T,z)\},$$

$$\{R_I(\mathbf{x}_{T1},\mathbf{x}_{T2},z)\} = \{L^1(\mathbf{x}_{T1},\mathbf{x}_{T1},\mathbf{x}_{T2},\mathbf{x}_{T2},z)\}.$$

We write $\mu(\mathbf{x})$ in the form $\mu(\mathbf{x}) = \bar{\mu}(\mathbf{x}) + \mu'(\mathbf{x})$ where $\bar{\mu}(\mathbf{x})$ represents the mean background profile and $\mu'(\mathbf{x})$ represents the random index of refraction fluctuations. We shall assume here that the statistics of the index-of-refraction field are homogeneous. The two-point correlation function, $\sigma(\mathbf{x}_1,\mathbf{x}_2)$, is defined as,

$$\sigma(\mathbf{x}_1,\mathbf{x}_2) = \{\mu'(\mathbf{x}_1)\,\mu'(\mathbf{x}_2)\}$$

and depends upon $\mathbf{r} = \mathbf{x}_1 - \mathbf{x}_2$. In addition, we define the function

$$\bar{\sigma}(\mathbf{x}_{T1} - \mathbf{x}_{T2}) = (1/4) \int_{-\infty}^{\infty} \sigma(\mathbf{x}_{T1} - \mathbf{x}_{T2}, r_z) dr_z.$$

B. Basic Equations

The moment equations for $\{\Gamma\}$ and $\{L^1\}$ in the anisotropic case are

$$\partial\{\Gamma\}/\partial z = (i/2k)[\nabla^2_{T1} - \nabla^2_{T2}]\{\Gamma\} -$$

$$k^2[\bar{\sigma}(0) - \bar{\sigma}(\mathbf{x}_{T1} - \mathbf{x}_{T2})]\{\Gamma\} +$$

$$ik[\bar{\mu}(\mathbf{x}_{T1}) - \bar{\mu}(\mathbf{x}_{T2})]\{\Gamma\}, \qquad (1)$$

$$\partial\{L^1\}/\partial z = (i/2k)[\nabla^2_{T1} - \nabla^2_{T2} - \nabla^2_{T3} + \nabla^2_{T4}]\{L^1\} +$$

$$k^2[\bar{\sigma}(\mathbf{x}_{T1} - \mathbf{x}_{T2}) + \bar{\sigma}(\mathbf{x}_{T1} - \mathbf{x}_{T3}) +$$

$$\bar{\sigma}(\mathbf{x}_{T2} - \mathbf{x}_{T4}) + \bar{\sigma}(\mathbf{x}_{T3} - \mathbf{x}_{T4}) -$$

$$\bar{\sigma}(\mathbf{x}_{T1} - \mathbf{x}_{T4}) - \bar{\sigma}(\mathbf{x}_{T2} - \mathbf{x}_{T3}) - \qquad (2)$$

$$2\,\bar{\sigma}(0)]\{L^1\} +$$

$$ik[\bar{\mu}(\mathbf{x}_{T1}) - \bar{\mu}(\mathbf{x}_{T2}) - \bar{\mu}(\mathbf{x}_{T3}) +$$

$$\bar{\mu}(\mathbf{x}_{T4})]\{L^1\}.$$

These equations are a direct generalization of the isotropic case in which the scalar separation distance r is replaced by the vector separation distance, $\mathbf{r}_{ij} = \mathbf{x}_{Ti} - \mathbf{x}_{Tj}$.

We have included in the above equations a mean background effect composed of a sum of $\bar{\mu}(\mathbf{x}_{T1})$ terms. It can easily be shown that, for a linear profile, this term has no real effect on our results. The measured patterns are simply displaced in position or angle.

For both the second- and fourth-order coherence functions, it is convenient to use a different set of independent coordinates. For the second-order case we transform to sum and difference coordinates defined as

$$\mathbf{p} = (\mathbf{x}_{T1} + \mathbf{x}_{T2})/2,$$
$$\mathbf{s} = (\mathbf{x}_{T1} - \mathbf{x}_{T2}). \tag{3}$$

In terms of **s** and **p**, Eq. (1) becomes

$$\partial\{\Gamma\}/\partial z = (i/k)\,\partial/\partial\mathbf{s} \cdot \partial/\partial\mathbf{p}\{\Gamma\} - k^2[\bar{\sigma}(0) - \bar{\sigma}(\mathbf{s})]\{\Gamma\}$$
$$+ ik[\,\bar{\mu}(\mathbf{p} + \mathbf{s}/2) - \bar{\mu}(\mathbf{p} - \mathbf{s}/2)]\{\Gamma\}. \tag{4}$$

For the fourth-order case, we transform to the coordinates

$$\mathbf{s} = (1/2)(\mathbf{x}_{T1} - \mathbf{x}_{T2} + \mathbf{x}_{T3} - \mathbf{x}_{T4}),$$
$$\mathbf{p} = (1/2)(\mathbf{x}_{T1} + \mathbf{x}_{T2} - \mathbf{x}_{T3} - \mathbf{x}_{T4}),$$
$$\mathbf{q} = (\mathbf{x}_{T1} - \mathbf{x}_{T2} - \mathbf{x}_{T3} + \mathbf{x}_{T4}),$$
$$\mathbf{R} = (1/4)(\mathbf{x}_{T1} + \mathbf{x}_{T2} + \mathbf{x}_{T3} + \mathbf{x}_{T4}). \tag{5}$$

Here,

$$\mathbf{r}_{12} = \mathbf{s} + \mathbf{q}/2 \qquad \mathbf{r}_{13} = \mathbf{p} + \mathbf{q}/2$$
$$\mathbf{r}_{14} = \mathbf{s} + \mathbf{p} \qquad \mathbf{r}_{23} = -\mathbf{s} + \mathbf{p}$$
$$\mathbf{r}_{24} = \mathbf{p} - \mathbf{q}/2 \qquad \mathbf{r}_{34} = \mathbf{s} - \mathbf{q}/2. \tag{6}$$

Using Eqs. (5) and (6), Eq. (2) may be written as

$$\partial\{L^1\}/\partial z = (i/k)\,[(\partial/\partial\mathbf{s}) \cdot (\partial/\partial\mathbf{p}) +$$
$$(\partial/\partial\mathbf{R}) \cdot (\partial/\partial\mathbf{q})]\{L^1\} + k^2\{\,\bar{\sigma}(\mathbf{r}_{12}) + \bar{\sigma}(\mathbf{r}_{13}) + \bar{\sigma}(\mathbf{r}_{24}) + \bar{\sigma}(\mathbf{r}_{34}) -$$
$$\bar{\sigma}(\mathbf{r}_{14}) - \bar{\sigma}(\mathbf{r}_{23}) - 2\bar{\sigma}(0)]\{L^1\} +$$
$$ik[\bar{\mu}(\mathbf{x}_{T1}) - \bar{\mu}(\mathbf{x}_{T2}) - \bar{\mu}(\mathbf{x}_{T3}) + \bar{\mu}(\mathbf{x}_{T4})]\{L^1\}. \tag{7}$$

C. Solutions

1. Plane Wave Boundary Condition: When there is no mean profile (i.e., $\bar{\mu} = 0$), Eq. (4) may be readily solved for an initial plane wave. In the plane wave case , the term $(\partial/\partial \mathbf{p})\{\Gamma\} = 0$ and the solution is

$$\{\Gamma(\mathbf{s},z)\} = I \exp(-k^2[\bar{\sigma}(0) - \bar{\sigma}(\mathbf{s})]z),$$

where I is the initial wave intensity. [If there is a linear profile, the right-hand side of Eq. (8) is multiplied by a phase term of the form exp (ikAsz), where the constant A is determined by the slope of the profile.]

The intensity is independent of z and this is readily confirmed by setting $\mathbf{s} = 0$. As |s| approaches infinity, we find

$$\{\Gamma(\infty,z)\} = I \exp(-k^2 \bar{\sigma}(0)z). \tag{9}$$

We may then interpret $\{\Gamma(\infty,z)\}$ as the intensity of the coherent field that remains after scattering. The quantity $L_f = 1/[k^2\bar{\sigma}(0)]$ is the characteristic distance over which signficant scattering occurs.

The perturbation solution for $\{R_I(\mathbf{x}_{T1},\mathbf{x}_{T2},z)\}$ obtained from Eq. (7) is

$$\{R_I(\mathbf{x}_{T1},\mathbf{x}_{T2},z)\} = I^2 [1 + (k^2z/2) \int_{-\infty}^{\infty}\int \tilde{\bar{\sigma}}(\mathbf{k}_{12}) \exp(i\mathbf{k}_{12} \cdot \mathbf{r}_{12})$$

$$(1 - (k/k_{12}^2z) \sin[k_{12}^2z/k])\, d\mathbf{k}_{12}] \tag{10}$$

where

$$\tilde{\bar{\sigma}}(\mathbf{k}_{12}) = (1/2\pi)^2 \int_{-\infty}^{\infty}\int \bar{\sigma}(\mathbf{r}_{12}) \exp(i\mathbf{k}_{12} \cdot \mathbf{r}_{12}) d\mathbf{r}_{12}.$$

A linear mean profile does not change the nature of this solution.

2. Point Source Boundary Condition: The solution for $\{\Gamma\}$ a point source is

$$\{\Gamma(\mathbf{s},z)\} = (I_z/z^2) \exp(-k^2z[\bar{\sigma}(0) - \int_0^1 \bar{\sigma}(a\mathbf{s})da]). \tag{11}$$

Here I_z is a normalization constant. Further discussion of this boundary condition will be given following the determination of the intensity distribution for a Gaussian beam boundary condition.

3. Gaussian Beam Boundary Condition: For $\bar{\mu} = 0$, Eq. (4) may be solved analytically for a Gaussian beam boundary condition For this case we have

$$\{\Gamma(\mathbf{x}_{T1},\mathbf{x}_{T2},0)\} = I \exp[-(|\mathbf{x}_{T1}|^2 + |\mathbf{x}_{T2}|^2)/2b^2]$$

$$= I \exp[-(|\mathbf{p}|^2 + |\mathbf{s}|^2/4)/b^2] \qquad (12)$$

The intensity, $\{I(\mathbf{p},z)\}$, is found to be

$$\{I(\mathbf{p},z)\} = (I\, b^2/4\pi) \iint_{-\infty}^{\infty} d\mathbf{w} \exp(-i\mathbf{w} \cdot \mathbf{p})$$

$$\exp[-w^2b^2(1 + z^2/k^2b^4)/4 + \bar{Q}(\mathbf{w},z)] \qquad (13)$$

where

$$\bar{Q}(\mathbf{w},z) = (k^3/w) \int_0^{wz/k} [\,\bar{\sigma}(w_x t/w, w_y t/w) - \bar{\sigma}(0,0)]dt. \qquad (14)$$

The only effect that a linear mean profile will have is to shift the maximum value of the intensity.

D. Computer Codes for the Direct Problem

We have written computer codes to evaluate Eq. (13) for the general anisotropic case and in the isotropic case. We have only to specify the function $\bar{\sigma}(\mathbf{r}_{ij})$ and the parameters k and b in order to find the intensity $\{I(\mathbf{p},z)\}$, as a function of separation distance $\mathbf{p}$, at range z. In Figs. 1 and 2 we show graphs of intensity vs. separation distance for $k = 420\ m^{-1}$ (100 Hz) and $b \approx 0.34$ m. The range is 500 m. The scattering function $\bar{\sigma}$ is chosen to be of the exponential form

$$\bar{\sigma}(w_x,w_y) = \{\mu'^2\}\, L_x \exp[-((|s_x|/L_x) + (|s_y|/L_y))], \qquad (15)$$

where we have chosen $\{\mu'^2\} = 10^{-9}$, the characteristic horizontal correlation length,

L_x = 100 m and the characteristic vertical correlation length, L_y = 1 m. The above numbers appear to be typical values for the fine structure, but are just meant here as an example. The exponential form was chosen somewhat arbitrarily since we could obtain simplified analytic solutions (presented below) to check the numerical program. We also performed some calculations using a Gaussian correlation function to further check the numerical code.

In Fig. 1 we have chosen $p_x = 0$ (to obtain a vertical intensity profile) and in Fig. 2 we took $p_y = 0$ (to obtain a horizontal intensity profile). As a result of the high anisotropy, the two profiles are very different. In fact, for the numbers chosen, the vertical profile is principally the result of scattering and the horizontal profile results principally from diffraction of the source. Note that the abcissas in Figs. 1 and 2 are different.

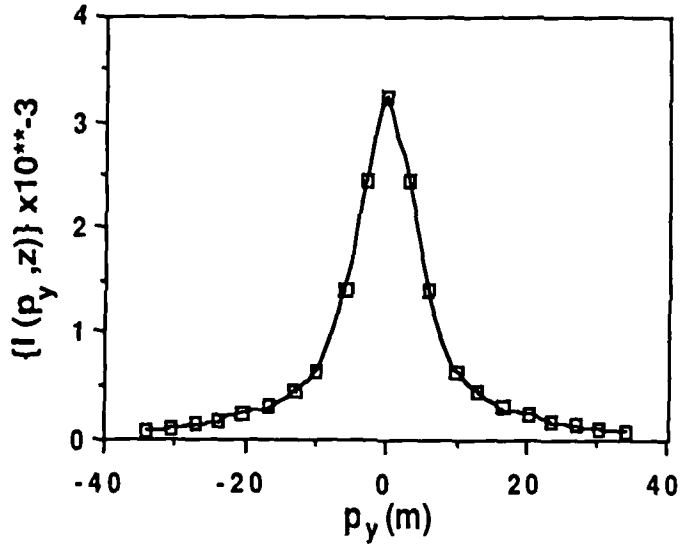

Fig. 1: Vertical Intensity Profile - I (p_y,z) vs p_y (p_x=0, k=420 m^{-1}, f=100 kHz, b=0.34m, $\{\mu_{12}\}=10^{-9}$, z=500 m)

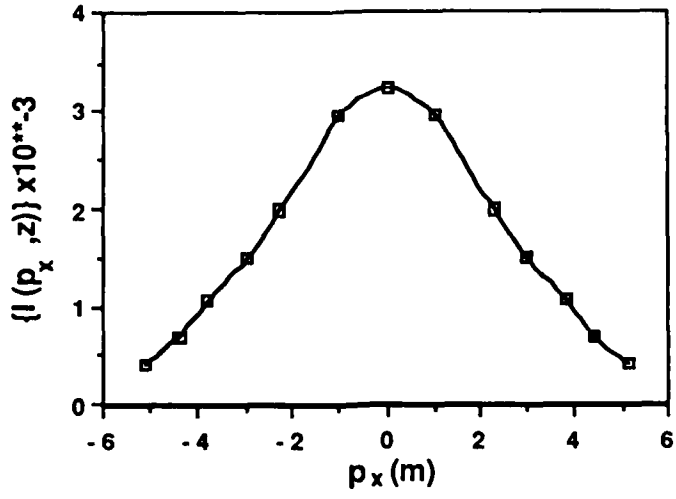

Fig. 2: Horizontal Intensity Profile - I (p_x,z) vs p_x (p_y=0, k=420 m^{-1}, f=100 kHz, b=0.34m, $\{\mu_{12}\}=10^{-9}$, z=500 m)

E. Analytic Approximation

The mean free path for scattering, L_f, is given by the expression

$$L_f = 1/(\{\mu'^2\}k^2L_x.$$

When the condition $z/L_f >> 1$ is satisfied, then the integral expression for $\bar{Q}(\mathbf{w},z)$, given in Eq. (14), can often be simplified. For the exponential correlation function (Eq. (15)), we find after some manipulation

$$\bar{Q}(\mathbf{w},z) = (1/2)\{\mu'^2\}kz^2[|w_x| + L_x|w_y|/L_y]. \qquad (16)$$

Using Eq. (16), the expression for $\{I(\mathbf{R},z)\}$ can be evaluated in terms of error functions. However, because of the condition $L_x/L_y >> 1$, we find that,for an under-ice Arctic experiment, we would anticipate diffraction of the source to dominate the intensity behavior in the horizontal (x) direction and scattering to dominate in the vertical (y) direction. Under these conditions we find, finally,

$$\{I(\mathbf{R},z)\}/I = [kb^3/\sqrt{\pi}\, z]\,[Kz^2/(K^2z^4 + R_y^2)]\,\exp[-(R_xkb/z)^2]\,, \qquad (17)$$

where $K = (1/2)\{\mu'^2\}kL_x/L_y$ and we have assumed that $z/kb^2 >> 1$.

In order to quickly assess the effect of changing frequency and range we can use Eq. (17). It must be emphasized, however, that the function $\{I(\mathbf{R},z)\}$ is very sensitive to

the form of $\bar{\sigma}$. Both the intensity at **R** = 0 and the characteristic decay length of theintensity in the vertical direction may change appreciably when the form of $\bar{\sigma}$ is changed.

For the values $\{\mu'^2\} = 4\{c'^2\}/\{c\}^2 = 10^{-9}$, L_x = 100 m and Ly = 1 m we present a small table for the characteristic vertical decay, R_{yc}, when $R_x = 0$. Here $z/L_f = 8.82$. The value of R_{yc} is taken at the point at which the intensity is half its initial value. From Eq. (17), we find,

$$R_{yc} = \{\mu'^2\}\, kL_x z^2/2L_y \qquad \theta_{yc} = R_{yc}/z.$$

z (m)	k (m^{-1})	R_{yc} (m)	θ_{yc} (rad)
300	420	1.89	0.0063
300	840	3.78	0.013
500	420	5.25	0.011
500	840	10.50	0.021
1000	420	21.00	0.021
1000	840	42.00	0.042

We note that R_{yc} and θ_{yc} depend on the parameters $\{\mu'^2\}$, L_x and L_y through the quantity $\bar{Q} = \{\mu'^2\}\, L_x/L_y$. In the above table, $\bar{Q} = 10^{-7}$. For example, if the anisotropy ratio, L_x/L_y, is 30 at the meter scales, rather than 100 as we have chosen above, all numbers in the right-hand two columns must be multiplied by .3. We note, however, that in this case $z/L_f = 2.65$, so that the analytic approximation is barely adequate. On the other hand, if $L_x/L_y = 10$, but at the same time we choose $\{\mu'^2\} = 10^{-8}$, rather than 10^{-9}, all numbers in the table remain the same and $z/L_f = 8.82$.

F. Point Source Boundary Condition - Determination of the Coherence Function

When the initial plane wave is replaced by a point source (all other parameters remaining the same), we find the result

$$\{\Gamma(\mathbf{s},z)\} = (I_z/z^2)\exp(-k^2 z[\,\bar{\sigma}(0) - \int_0^1 \bar{\sigma}(a\mathbf{s})\,da]. \qquad (18)$$

Here, I_z is a normalization constant. Apart from the z^2 decay, the above formula differs from the plane wave case by the replacement of $\bar{\sigma}(\mathbf{s})$ by the integral in the exponent. It is convenient to do calculations in the following normalized form:

$$\{\bar{\Gamma}(\mathbf{s},z)\} = \{\Gamma(\mathbf{s},z)\}/(l_z/z^2)$$

$$= \exp[-(1 - (1/\bar{\sigma}(0))(\int_0^1 \bar{\sigma}(a\mathbf{s})\, da)(z/L_f))], \tag{19}$$

where $L_f = 1/[k^2 \bar{\sigma}(0)]$. Here $\bar{\sigma}(0) = \{\mu'^2\}L_x$.

Choosing the following typical values,

$k = 420\ m^{-1}$,
$L_x = 100$ m,
$\{\mu'^2\} = 10^{-9}$,
$z = 500$ m,

we have $z/L_f = 8.8$. This means we are in the strong scattering region. If L_x and $\{\mu'^2\}$ are approximately correct, then only by decreasing the signal frequency or reducing the range can we move out of this region. However, for the previous theory to be correct we require z/L_x to be at least greater than three.

From a computational point of view, it is desirable to be in the strong scattering region (as we shall see below). The disadvantage is that, in this case, one can only determine the smaller length scales in $\bar{\sigma}(\mathbf{s})$. The larger scales have little effect in this regime.

If the correlation function is of the exponential form

$$\bar{\sigma}(a\mathbf{s}) = \exp(-a|s_x|/L_x - a|s_y|/L_y) \tag{20}$$

we find

$$\{\bar{\Gamma}(\mathbf{s},z)\} = \exp\{-[1 - (1/(|s_x|/L_x + |s_y|/L_y)(1 - \exp-(|s_x|/L_x + |s_y|/L_y))](z/L_f)\} \tag{21}$$

When $z/L_f >> 1$, only those values of $\mathbf{s}$ for which $|s_x|/L_x$ and $|s_y|/L_y$ are much less than unity contribute significantly to $\{\bar{\Gamma}(s)\}$. In this case, we may expand the exponential $\exp -(|s_x|/L_x + |s_y|/L_y)$ in a power series and we will find, finally

$$\{\bar{\Gamma}(\mathbf{s},z)\} = \exp[-(|s_x|/L_x + |s_y|/L_y)(z/L_f)]. \tag{22}$$

The angular power spectrum associated with $\{\Gamma(\mathbf{s},z)\}$ is defined as

$$\{\tilde{\Gamma}(\kappa,z)\} = \int_{-\infty}^{\infty}\int \exp[i\kappa \cdot \mathbf{s}]\{\Gamma(\mathbf{s},z)\}ds_x ds_y,$$

and we find, using Eq. (22),

$$\{\tilde{\Gamma}(\kappa,z)\} = \frac{4(2L_f/z)^2 L_x L_y}{[(2L_f\kappa_x L_x/z)^2 + 1]\,[(2L_f\kappa_y L_y/z)^2 + 1]}. \tag{24}$$

From Eq. (24) we see that the characteristic scattering angle in the vertical direction is of the order of $\theta_y/k = (z/L_f)(1/2kL_y)$. This result is the same as that obtained for the quantity $\theta_{yc} = R_{yc}/z$ for the spread of a Gaussian beam. Thus, we see that we obtain the same type of information if we measure either the intensity distribution of a Gaussian beam or the coherence function associated with a point source. In view of the expected experimental errors, it would be most desirable to measure both quantities simultaneously.

In the literature, it is often postulated that the wave number spectra in the horizontal and vertical directions obey inverse power laws of the form

$$W(\kappa_i) = [\Gamma(\nu_i + 1/2)L_i/\sqrt{\pi}\,\Gamma(\nu_i)]$$

$$[1/(1 + (\kappa_i L_i)^2]^{(\nu_i + 1/2)}. \tag{25}$$

The normalization is chosen so that $\bar{\sigma}(0) = 1$. Here $\Gamma(\nu_i)$ denotes a Gamma function.

We then find that $D(s_i) = [\bar{\sigma}(0) - \bar{\sigma}(s_i)]$ is equal to

$$D(s_i) = [1 - 2^{(1-\nu)}(1/\Gamma(\nu_i))\,(s_i/L_i)^{\nu_i} K_{\nu_i}(s_i/L_i)] \tag{26}$$

In the strong scattering limit we find, then

$$\{\Gamma(\mathbf{s},z)\} = \exp[-(B\nu_x)(|s_x|/L_x)^2 + B(\nu_y)(|s_y|/L_y)^{2\nu_y})(z/L_f)] \tag{27}$$

where

$$B(\nu_i) = \Gamma(1 - \nu_i)/\Gamma(1 + \nu_i)(2\nu_i + 1)2^{\nu_i}. \tag{28}$$

For $\nu_i = 1/2$, we find Eq. (22). A few values of $B(\nu_i)$ are:

ν_i	$B(\nu_i)$
0.500	0.500
0.625	0.494
0.750	0.558
0.875	0.854.

If $\nu_i = 1$ then B diverges.

There is no simple analytic expression for the spectrum $\{\tilde{\Gamma}(\kappa,z)\}$. However, it is a simple matter to evaluate the function numerically.

G. Inversion Formulas

The inversion formulas needed to determine $\bar{\sigma}(\mathbf{s})$ from either $\{\Gamma\}$ or $\{I\}$ are direct extensions of the methods used for the isotropic case. In this section, we shall consider the following cases:

1. Measurement of $\{\Gamma\}$ for a plane wave boundary condition.
2. Measurement of $\{\Gamma\}$ for a point source boundary condition.
3. Measurement of $\{I\}$ for a gaussian beam boundary condition.
4. Measurement of $\{R_I\}$ for a plane wave boundary condition.

1. Plane wave boundary condition for $\{\Gamma\}$:

Direct solution:

$$\{\Gamma(\mathbf{s},z)\} = I \exp(-k^2[\bar{\sigma}(0) - \bar{\sigma}(\mathbf{s})]\, z) \tag{29}$$

Inverse solution:

$$\bar{\sigma}(\mathbf{s}) = \bar{\sigma}(0) + (1/k^2 z) \log[\{\Gamma(\mathbf{s},z)\}/I] \tag{30}$$

or

$$\bar{\sigma}(\mathbf{s}) = (1/k^2 z) \log[\{\Gamma(\mathbf{s},z)\}/\{\Gamma(\infty,z)\}]. \tag{31}$$

2. Point source boundary condition for $\{\Gamma\}$:

Direct solution:

$$\{\Gamma(\mathbf{s},z)\} = (I_z/z^2)\exp(-k^2z[\bar{\sigma}(0) - \int_0^1 \bar{\sigma}(a\mathbf{s})da]) \tag{32}$$

Inverse solution:

$$\int_0^1 \bar{\sigma}(a\mathbf{s})da = \bar{\sigma}(0) + (1/k^2z)\log[\{\Gamma(\mathbf{s},z)\}/(I_z/z^2)]. \tag{33}$$

The coordinates s_x and s_y may be any orthogonal coordinates in the transverse plane. To reduce Eq. (33) to an expression for $\bar{\sigma}(\mathbf{s})$, we choose one of the $\mathbf{s}$ coordinates equal to zero. For example, we take here $s_y = 0$. Next, noting that

$$d/ds_x[\, s_x \int_0^1 \bar{\sigma}(as_x)da] = \bar{\sigma}(s_x)$$

we find the following expression for $\bar{\sigma}(s_x)$

$$\bar{\sigma}(s_x) = \bar{\sigma}(0) +$$

$$d/ds_x[(s_x/k^2z)\log(\{\Gamma(s_x,z)\}/(I_z/z^2))] \tag{34}$$

or

$$\bar{\sigma}(s_x) = d/ds_x[(s_x/k^2z)\log(\{\Gamma(s_x,z)\}/\{\Gamma(\infty,z)\})]. \tag{35}$$

There is a similar expression for s_y when $s_x = 0$.

3. Gaussian source boundary condition for $\{I\}$:

Direct solution:

$$\{I(\mathbf{p},z)\} = (I\, b^2/4\pi)\iint_{-\infty}^{\infty} d\mathbf{w}\ \exp(-i\mathbf{w}\cdot\mathbf{p})\exp[-w^2b^2(1 + z^2/k^2b^4)/4 + \bar{Q}(\mathbf{w},z)] \tag{36}$$

where

$$\bar{Q}(\mathbf{w},z) = (k^3/w)\int_0^{wz/k} [\,\bar{\sigma}(w_x t/w, w_y t/w) - \bar{\sigma}(0,0)]dt. \tag{37}$$

Here, $\{I(\mathbf{p},0)\} = I \exp[-p^2/b^2]$.

Inverse solution:

$$\bar{Q}(\mathbf{w},z) = w^2b^2(1 + z^2/k^2b^4)/4 + \log[1/(I\, b^2\pi)\iint_{-\infty}^{\infty} \{I(\mathbf{p},z)\} \exp(i\mathbf{w}\cdot\mathbf{p})d\mathbf{p}]. \tag{38}$$

To find $\bar{\sigma}$ from $\bar{Q}$ along one of the transverse axes, we set one of the orthogonal coordinates of **w** equal to zero, say $w_y = 0$. We find, then, from Eq. (37)

$$\bar{\sigma}(w_x z/k,0) = \bar{\sigma}(0,0) + (1/k^2 z)[\partial(w_x \bar{Q}(w_x,0,z))/\partial w_x]. \tag{39}$$

There is a similar expression for w_y when $w_x = 0$. Moreover, by suitable rotation of the transverse coordinate axes, we may find $\bar{\sigma}$ along any axis. The coupling between coordinate axes in $\bar{\sigma}$ may be obtained by keeping **w** arbitrary and differentiating Eq. (37) with respect to the vector magnitude, w. The expression is then

$$\bar{\sigma}(\mathbf{w}z/k) = \bar{\sigma}(0,0) + (1/k^2 z)[\partial(w\bar{Q}(\mathbf{w},z))/\partial w]. \tag{40}$$

4. Plane wave boundary condition for $\{R_I\}$:

Direct Solution:

The perturbation solution for $\{R_I(\mathbf{x}_{T1},\mathbf{x}_{T2},z)\}$ is

$$\{R_I(\mathbf{x}_{T1},\mathbf{x}_{T2},z) = I^2 [1 + (k^2 z/2)\iint_{-\infty}^{\infty} \tilde{\bar{\sigma}}(\mathbf{k}_{12}) \exp(i\mathbf{k}_{12}\cdot\mathbf{r}_{12})$$

$$(1 - (k/k_{12}^2 z)\sin[k_{12}^2 z/k])d\mathbf{k}_{12}], \tag{41}$$

where

$$\bar{\tilde{\sigma}}(\mathbf{k}_{12}) = (1/\pi)^2 \iint_{-\infty}^{\infty} \bar{\sigma}(\mathbf{r}_{12}) \exp(i\mathbf{k}_{12} \cdot \mathbf{r}_{12}) d\mathbf{r}_{12}.$$

From Eq. (41), we see that $\{R_I\}$ is determined by a rather complicated integral of the function $\bar{\tilde{\sigma}}(\mathbf{k}_{12})$. However, this integral reduces to a simplified relation in two limits: (1) in the geometric optics region where $z << ks_c^2$ (s_c is the smallest characteristic length associated with the coherence function) and, (2) when $z >> ks_c^2$. In the geometric scattering region we find

$$\{R_I(\mathbf{x}_{T1},\mathbf{x}_{T2},z) = I^2 [1 + (1/12)(z^3) \iint_{-\infty}^{\infty} \bar{\tilde{\sigma}}(k_{12})(k_{12}^4) \exp(i\mathbf{k}_{12} \cdot \mathbf{r}_{12}) d\mathbf{k}_{12}],$$

$$= I^2 [1 + (1/3) z^3 \nabla^4 \bar{\sigma}(\mathbf{r}_{12})]. \quad (42)$$

When $z >> k\mathbf{s}_c^2$,

$$\{R_I(\mathbf{s},z)\} = I^2 [1 + (k^2 z/2) \iint_{-\infty}^{\infty} \bar{\tilde{\sigma}}(k_{12}) \exp(i\mathbf{k}_{12} \cdot \mathbf{r}_{12}) d\mathbf{k}_{12}]$$

$$= I^2 [1 + 2k^2 z \, \bar{\sigma}(\mathbf{r}_{12})]. \quad (43)$$

Inverse solution:

For $z << ks_c^2$ we find

$$\nabla^4 \bar{\sigma}(\mathbf{r}_{12}) = (3/z^3)[R_I(\mathbf{r}_{12},z) - I^2]/I^2. \quad (44)$$

For $z >> ks_c^2$,we have

$$\bar{\sigma}(\mathbf{r}_{12}) = (1/2k^2 z)[R_I(\mathbf{r}_{12},z) - I^2]/I^2. \quad (45)$$

III. Application of the Theory to the Arctic Environment

To properly design and evaluate an experiment to be conducted under Arctic ice , it is desirable to have some idea of the scattering properties of the Arctic Ocean environment. Despite an extensive search of the literature, very little data was found for the meter-to-centimeter scales in which we are interested. Not only is the shape of the correlation function (or associated wave number spectrum) largely unknown, but the relevant length and intensity scales can be estimated at best only to within an order of magnitude. The best information that we have been able to obtain is given in the references at the conclusion of this section.

For purposes of estimating effects of the fine structure in the ocean we have assumed the values of the ratio $\{c'^2\}/\{c\}^2$ (the ratio of mean square sound-speed flucuations to the mean sound-speed squared) to be of the order of 10^{-10} to 10^{-9}. The vertical correlation length is taken to be 1-3 meters, with the horizontal correlation length about 10 to 100 times the vertical correlation length. Typical results using these numbers are given in Section II.

References

(1962) H. L. Grant, R. W. Stewart and A. Moilliet, Turbulent spectra from a tidal channel, J. Fluid Mech. 12, 241-268

(1964) R. F. Shvachko, Sound fluctuations in the upper layer of the ocean and their relation to random inhomogeneities of the medium, Sov. Phys. - Acoust., 9, 280-282

(1967) R. F. Shvachko, Sound fluctuations and random inhomogeneities in the ocean, Sov. Phys. - Acoust., 13, 93-97

(1974) T. R. Osborn, Vertical profiling of velocity microstructure, J. Phys. Ocean. 4, 109-115

(1975) A. E. Gargett, An investigation of the occurence of oceanic turbulence with respect to finestructure, J. Phys. Ocean. 6, 139-156

(1979) S. M. Flatte, R. Dashen, W. H. Munk, K. M. Watson, F. Zachariasen, Sound Transmission Through a Fluctuating Ocean (Cambridge University Press, Cambridge)

(1983) N. S. Oakey, Determination of the rate of dissipation of turbulent energy for simultaneous temperature and velocity shear microstructure measurements, J. Phys. Ocean., 12, 256-271

(1985) M. D. Levine, C. A. Paulson and J. M. Morison, Internal waves in the Arctic: Comparison with lower-latitude observations, J. Phys. Ocean., 15, 800-809

(1985) L. Nghiem-Phu and F. Tappert, Parabolic equation modeling of the effects of ocean currents on sound transmission and reciprocity in the time domain, J. Acoust. Soc. Amer. 78, 642-648

(1985) T. R. Osborn and R. G. Lueck, Turbulent measurements with a submarine, J. Phys. Ocean. 15, 1502-1520

(1985) J. S. Robertson, W. L. Siegman and M. J. Jacobson, Current and current shear effects in the parabolic approximation for underwater sound channels, J. Acoust. Soc. Amer. 77, 1768-1780

(1985) M. Schulkin, G. R. Garrison and T. Wen, High frequency acoustic variability in the Arctic, J. Acoust. Soc. Amer., 77, 465-481

IV. Effect of Random Velocity Fluctuations on Underwater Scattering

There is a well-developed theory to account for the effect of random fluctuations in the sound-speed on the underwater scattering of acoustic radiation. In Appendix A, we show how the theory may be extended to include the effect of random fluctuations in fluid velocity. We assume that the characteristic time and length scales associated with the velocity correlation functions are long when compared to the corresponding scales (period and wave length) of the acoustic radiation.

The importance of fluid velocity fluctuations depends upon the scale sizes of importance in any acoustic experiment. For experiments in which internal waves have the dominant effect on acoustic fluctuations, the fluid velocity fluctuations may be neglected. However, for experiments in which the fine structure plays a dominant role, fluid velocity fluctuations begin to have an effect. In the paper included as Appendix A we show how the fluid velocity fluctuations may be taken into account using the inverse method proposed for the arctic experiment. More standard methods require direct measurement of the fluid velocity fluctuations; a procedure that is exceptionally difficult and rarely reported in the literature.

V. Determination of the Intensity Distribution from a Circular Source in an Isotropic Random Medium

In a paper by Whitman and Beran (1970), the intensity distribution was determined for a Gaussian beam propagating in an isotropic random medium. Here, we present a similar result for a circular source (i.e. constant intensity for a radial distance less than the radius a and zero for greater radial distances). The difficulty in the calculation is determining the initial coherence function, since the initial field is discontinuous. We shall first outline the method of solution and then determine the initial coherence function. Finally, we present the integral that must be evaluated to determine the intensity.

A. Method of Solution

The basic equation for the coherence function, $\{\Gamma\}$, is

$$\partial\{\Gamma\}/\partial z = (i/k)\,\partial/\partial \mathbf{s} \cdot \partial \mathbf{p}\{\Gamma\} + k^2 F(s)\{\Gamma\}, \tag{46}$$

where z is the range, **p** is the mean transverse coordinate, **s** is the transverse difference coordinate and k is the wave number. The function F(s) is given by the expression

$$F(s) = [\bar{\sigma}(s) - \bar{\sigma}(0)]$$

where $\bar{\sigma}(s)$ is the transverse correlation function associated with the index-of-refraction fluctuations.

To solve Eq. (46), we take the double Fourier transform with respect to **p**. The result is

$$\partial\{\Gamma\}/\partial z - (1/k)\mathbf{u} \cdot \partial/\partial\mathbf{s}\{\Gamma\} - k^2F(s)\{\Gamma\} = 0. \tag{47}$$

We solve Eq. (47) by the method of characteristics. The result is, (after some manipulation),

$$\{I(u,z)\} = \{\Gamma(\mathbf{u_o},\mathbf{s_o},0)\} \exp[k^2 \int_0^z F(uq/k)dq] \tag{48}$$

where $\mathbf{s_o} = -\mathbf{u_o}z/k$ and $\mathbf{u} = \mathbf{u_o}$. The intensity is found from $\{I(u,z)\}$ from the Bessel transform relation

$$\{I(R,z)\} = (1/2\pi) \int_0^\infty \{I(u,z)\} J_o(uR)udu. \tag{49}$$

B. Determination of the Initial Coherence Function

In terms of the initial field, $V(\mathbf{x})$, we have

$$\{\Gamma(\mathbf{u_o},\mathbf{s_o},0)\} = \iint_{-\infty}^{\infty} \exp[i\mathbf{u_o} \cdot \mathbf{p_o}]\, V(\mathbf{p_o} + \mathbf{s_o})\, V^*(\mathbf{p_o})d\mathbf{p_o}. \tag{50}$$

Using the convolution theorem, this yields

$$\{\Gamma(\mathbf{u_o},\mathbf{s_o},0)\} = (1/2\pi)^2 \iint_{-\infty}^{\infty} \exp[-\mathbf{s_o} \cdot \mathbf{t}]W(\mathbf{t})\, W^*(\mathbf{t} + \mathbf{u_o})d\mathbf{t}, \tag{51}$$

where

$$W(\mathbf{t}) = \iint_{-\infty}^{\infty} \exp[i\mathbf{t} \cdot \mathbf{p_o}]\, V(\mathbf{p_o})d\mathbf{p_o}. \tag{52}$$

For a circular source, we find

$$W(t) = I_o\, 2\pi a\, J_1(at)/t. \tag{53}$$

Since the function $\{\Gamma(\mathbf{u_o},\mathbf{s_o},0)\}$ depends only on u_o, we use the simplified notation

$$I_s(u_o,o) = \{\Gamma(\mathbf{u_o},\mathbf{s_o},0)\}$$

and find, finally,

$$I_s(u_o,o) = a^2 \int_0^{\infty}\int_0^{2\pi} \exp[iu_o t \cos(v)\, z/k]\, J_1(at)/t$$

$$J_1[a(t^2 + u_o^2 + 2t\, u_o \cos(v))^{1/2}]$$

$$1/(t^2 + u_o^2 + 2t\, u_o \cos(v))^{1/2} dt\, dv. \qquad (54)$$

The final solution is then

$$\{I(u,z)\} = I_s(u,0) \exp[k^2 \int_0^z F(uq/k)dq], \qquad (55)$$

where $I_s(u_o,0)$ *is given by* Eq. (54) (here $u = u_o$) and $\{I(R,z)\}$ is then found using Eq. (49).

We note that, in the far field $z \to \infty$, only values of $u_o/k<<1$ are important, and we determine that

$$I_s(u_o,o) = I_o\, 2\pi a^2 \int_0^{\infty} [J_1(at)/t]^2\, J_o(u_o tz/ak)tdt. \qquad (56)$$

References

(1970) A.M. Whitman and M. Beran, Beam spread of laser light propagating in a random medium. J.Opt.Soc.Amer. 60, 1595-1602

VI. Studies of the Optimum Parameters for a Tank Experiment

As a part of our work, we attemped to conduct a limited validation of the theory presented. In order to acomplish this within the scope of this current contract, we performed an experiment in which we scattered sound from artificially generated sound speed inhomogenieties in a large laboratory tank. In designing this experiment, we needed to determine the correlation function associated with the sound-speed fluctuations, using the inverse method. In order to do this, the effect of scattering must be stronger than source diffraction effects, but not so strong that only the very smallest scales of the fluctuations are important. The optimum conditions occur when the the strength parameter B defined below, is of order unity and the ratio s/a (scattering to diffraction effect) is as large as possible.

A. Temperature Fluctuations

While the ultimate parameter of interest was the sound speed, cost considerations led us to measure the temperature of the water and then to compute sound speed for zero salinity (tap) water. The relationship between the temperature and sound speed fluctuations may be determined from the following well known relation between sound speed c and temperature T.

$$c = 1449.0 + 4.6\,T - 0.055\,T^2 + 0.0003\,T^3,$$

where c is in m/sec and T is in degrees Centigrade. Taking the differential of the above equation yields

$$dc = 4.6\,dT - 0.11\,dT + 0.0009\,T^2\,dT.$$

For $T = 25^0$ C, a typical tank temperature,

$$dc = 2.25\,dT.$$

For $dT = 1^0$ C, $dc/c = 0.0015$ and $\mu^2 = 4(dc/c)^2 = 9 \times 10^{-6} = 10^{-5}$; $\mu^2 = \{\mu'^2\}$.

B. Strength of Scattering

The strength of scattering B may be defined as follows

$$B = \mu^2 k^2 / z$$

where k is the radiation wavenumber (m^{-1})and for a frequency of f=1 MHz, ($k = 4200\ m^{-1}$) , l is the characteristic turbulent correlation length and z is the path length (m).

Typical values are as follow.

$k(m^{-1})$	μ^2	l(m)	z(m)	B	$B^{1/2}$
4200	10^{-5}	.1	3	52.90	7.27
4200	10^{-5}	.01	3	5.29	2.30
2100	10^{-5}	.01	3	1.32	1.15
2100	10^{-5}	.03	3	3.97	1.99
4200	10^{-6}	.03	3	1.59	1.26
2100	10^{-6}	.03	3	0.40	0.63

C. Angle of Scattering and Spread

Single scattering angle, $\theta_{TS} = (1/kl)$.

Multiple scattering angle, $\theta_T = B^{1/2}(1/kl)$.

Spread, $s = (\theta_T)z$.

D. Fresnel Region

For a Gaussian source, the diffraction effect is a minimum at a distance z if the source size a is chosen so that $a = (z/k)^{1/2}$.

Typical values are shown below.

z(m)	$k(m^{-1})$	a(m)	ka
3	4200	0.0267	112.2
3	2100	0.0378	79.4

E. Ratio s/a

The ratio $s/a = [Bz/k\ell^2]^{1/2}$ gives us the relative importance of turbulent scattering to source diffraction. Some typical values are given below.

Table I

$k(m^{-1})$	μ^2	ℓ(m)	z(m)	B	$B^{1/2}$	s/a
8400	10^{-5}	0.1	3	211.600	14.540	2.740
8400	10^{-6}	0.1	3	21.600	4.600	0.866
8400	10^{-7}	0.1	3	2.120	1.450	0.274
8400	10^{-5}	0.03	3	63.600	8.000	7.140
8400	10^{-6}	0.03	3	6.360	2.520	2.250
8400	10^{-7}	0.03	3	0.636	0.800	0.710
8400	10^{-5}	0.01	3	21.160	4.600	8.680
8400	10^{-6}	0.01	3	2.120	1.450	2.740
8400	10^{-7}	0.01	3	0.212	0.460	0.866
4200	10^{-5}	0.1	3	52.900	7.270	1.940
4200	10^{-6}	0.1	3	5.290	2.300	0.613
4200	10^{-7}	0.1	3	0.529	0.727	0.194
4200	10^{-5}	0.03	3	15.900	3.990	5.020
4200	10^{-6}	0.03	3	1.590	1.260	1.590
4200	10^{-7}	0.03	3	0.159	0.399	0.502
4200	10^{-5}	0.01	3	5.290	2.300	6.140
4200	10^{-6}	0.01	3	0.529	0.727	1.940
4200	10^{-7}	0.01	3	0.053	0.230	0.614
2100	10^{-5}	0.1	3	13.200	3.630	1.370
2100	10^{-6}	0.1	3	1.320	0.363	0.137
2100	10^{-5}	0.03	3	3.970	1.990	2.510
2100	10^{-6}	0.03	3	0.400	0.630	0.800
2100	10^{-7}	0.03	3	0.040	0.200	0.253
2100	10^{-5}	0.01	3	1.320	1.150	4.340
2100	10^{-6}	0.01	3	0.132	0.363	1.370
2100	10^{-7}	0.01	3	0.013	0.115	0.434

The best situation, from an inversion point of view, is B near unity and s/a as high as possible. As we stated above, the reason to require that the value of B is close to one is to insure that all scales of the turbulence contribute to the intensity pattern. If B is very large, only the very small scales are important. On the other hand, if $B<<1$, then the turbulence does not have much effect.

VII. Laboratory Tank Experiment

A prototype experiment was conceived and executed with the objective of at least partially validating the theory presented in the preceding part of this report. The experimental protocol was heavily influenced by the availability of certain instrumentation and computer data acquisition interfaces. Only with the use of those resources could we hope to accomplish the objective of comparing theory and experiment within our existing funding resources.

Basically, the experiment was designed in two parts. The first involved measurement of the correlation function for an artificially induced heterogeneous spatial structure in the speed of sound. The structure was created in two ways. One involved the placement of a heater grid on the tank bottom. A thin plastic sheet was placed over this heater grid. Holes had been punched (ca 1 cm diameter) randomly in the sheet in a position that was directly under the projected sound propagation path. The density of these holes, through which the heated water rose (due to its own density contrast with the surrounding water) was 2000 / m^2. The second technique involved a reversal of the process described above. Ice was floated in the water above a second sheet that was similiar to that described for the heater. As the cold water sank, it was introduced into the propagation path. Not suprisingly, as the experimental tank is outdoors, the heater resulted in the strongest sound speed heterogeneity in the experiments conducted in the winter when the ambient tank temperature was about 8^{0}C, and the melting ice was most effective in the summer and fall when ambient air temperatures were higher (ca 20-23^{0}C). On occasion, when the ambient temperature was intermediate (ca 14^{0}C), and a strong scattering field was desired, both techniques were used simultaneously.

A. Sound Speed

The sound speed was computed from measurements of the water temperature at six points separated by 1 cm along a horizontal line. Since tap water was used in the tank, the salinity was assumed to be sufficiently close to zero to justify an assumption that it could be neglected both on the average and in terms of the spatial heterogeneity that it might introduce. The thermistors used were calibrated to an accuracy of 0.01^{0}C in an oil bath. The time constant for these thermistors had been previously measured and were found to be ca 8 ms in water (1/e). A regulated voltage source was used to excite each thermistor and the resulting voltages were digitized by independent auto-zeroing A/D converters. The circuit was designed to automatically compensate for any fluctuations in the source voltage by use of a ratiometric technique.

The A/D converters (12-bit) were strobed to begin their conversions simultaneously and the digitized data were latched for transfer to the data acquisition computer as soon as each set of conversions was completed. Thus, a complete set of independent temperatures was available at a 30 Hz rate. These binary representations of the temperature at each thermistor were transfered to the data acquisition computer as a serial sequence of bytes. There they were stored in a RAM buffer until the required data sequence was completed. At that time the numbers were converted to engineering units (^{0}C) and stored on a floppy disk. An option was provided for deleting unwanted data from the data stream before storing in the buffer if

the full sampling rate of 30 Hz was not desired. This procedure was implemented by the simple process of skipping the storage of data sets between desired sample times.

The data were displayed in both a columnar format on a CRT and optionally on a printer and as a plot on a graphic display. The temperature data were then converted to sound speed and the correlation function for that parameter was also made available in both numerical and graphical display formats.

B. Fluctuations in the Received Acoustic Pulses

Acoustic pulses were projected over a path of 2.33 m at a depth of 1 m in the tank. The water depth was maintained at just under 2 m. The tank is 2 m (deep) by 2 m (width) by 4 m (length). A pulse length of 1 ms was used and the acoustic center frequency was 0.925 MHz. The projector, a transducer constructed from a PVDF (polyvinylidene fluoride) film of 110 μm thickness was fabricated as five concentric rings. The outer diameter of the largest ring was 10 cm. The drive voltage to these rings was shaded in an approximation to a Gaussian curve with a resistive network. The resultant beam pattern was a good approximation to a Gaussian shape inside the $^1/_e$ points on the intensity pattern. Beyond that point, however, the approximation deviated from a Gaussian shape, falling off too rapidly. It is possible that this deviation was due to an uncompensated reactive component of the cable and shading network at this (relatively high) frequency. This kind of error is layout sensitive, and can not be modeled to allow ready correction. It can be adjusted by an iterative approach, however, our time and resources did not permit this to be accomplished for this task.

Two small probe hydrophones, one a disk (ca 2.5 cm diameter and the other a cylinder (1.1 cm height and 0.7 cm outer diameter) were located at the same depth as the source at a distance of 2.33 m. The disk was fixed relative to the transmitted sound beam and the cylinder could be adjusted in the horizontal in a direction that was orthogonal to the undistorted direction of travel of the source's main lobe.

In any acoustics experiment to be conducted in a finite sized tank, one must be concerned with the potential impact of reflections on the received signals. In particular, at the frequencies with which we were concerned in this experiment, modulation of the surface reflected path by small ripples would have interfered with our ability to discriminate forward scattering induced reflections. In order to assure that surface reflections would not be present in our measurements, we: 1) chose to work with as short a pulse as was practical (< 1 ms), 2) used a range gate to assure that the measurement included only the direct arrival and those (relatively) small variations due to forward volume scattering rather than signals reflected from the water surface, the tank walls or bottom, 3) used the directivity of the receiving hydrophones to reject energy arriving at the range gate during the sampling period at large vertical angles off their pointing direction and, 4) transmitted at a rate (ca 1/sec) that assured that the reverberation in the tank from previous transmissions had been sufficiently attenuated before the next sequence began.

A bandpass filter centered at 0.925 MHz was used to reject electronic noise (principally from commercial radio stations in this band) and thermal noise that fell outside the desired band around the acoustic transmission frequency. The energy in

the range gate was integrated over the duration of the gate, the output sampled held and digitized by an A/D converter (12-bit). The result was transfered to the data acquisition computer for storage on floppy disks and for display both in numerical and in graphical form.

The normalized intensity distributions, scintillation indices (variance of the intensity fluctuations) and the correlation function of the intensities were computed and displayed as functions of the separations between the two probe hydrophones.

VIII. Analysis of the Tank Experiment Results

The experimental results obtained demonstrate that under laboratory conditions, it is feasible to measure, both the correlation function of the sound-speed fluctuations and the intensity distribution of a beam that has traversed a heterogeneous medium. This means that it is possible both to study the validity of the basic theory that has been developed to predict the intensity distribution and to determine the utility of the inverse procedure discussed in the previous sections. We have shown that it is possible to obtain values of μ^2 of the order of 10^{-7} in the laboratory. For this value of μ^2, significant scattering of a beam occurs and the scattering effect may be distinguished from the diffraction effect. In addition, it has been possible to measure the correlation of intensities so that measured values of the scintillation index may also be compared to those predicted by theory.

An example of a measured sound-speed correlation function is given in Fig. 3. The characteristic correlation length is about 1 cm and $\mu^2 = 0.806 \times 10^{-6}$. By changing the heating or cooling in the tank μ^2 may vary between 10^{-8} and 10^{-6}. Thus, we can meet the conditions that B is approximately unity and s/a > 1. See, for example, $k = 4200\ m^{-1}$, $l = 0.01$ and 0.03, $\mu^2 = 10^{-6}$ in Table I.

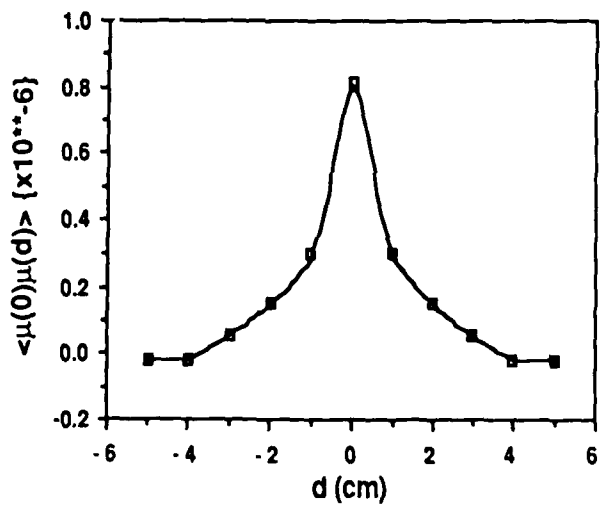

Fig. 3: Sound Speed Correlation Function vs. Separation Distance

In Table II, we show normalized intensity distributions that were measured under weak turbulence conditions ($\mu^2 = 0.5 \times 10^{-7}$) and strong turbulence conditions ($\mu^2 = 0.806 \times 10^{-6}$). We see, from comparison of the intensity distributions, that the beam in the strong turbulence case was wider. In this feasibility experiment, the absolute intensities were not measured (though this could be done by calibrating the probe hydrophones by a reciprocity or a comparison technique). We did not measure

the intensity reduction on the beam axis in the current effort. The beam shape departed too far from Gaussian beyond the 1/e - point to make it useful to carry out an inverse calculation on these data.

In future work, we have two choices. We can either devote considerable more effort to making the skirts of the beam distribution more nearly Gaussian (a tedious, but achievable goal) or we can fully develop a theory for a beam with a more general beam shape. Since the natural shape of lines and disks involve the appropriate Bessel functions, a model for such a beam was considered on a theoretical basis and seems practical. However, the numerical calculations for a non-Gaussian beam was not within the scope of the current work. In either case, the theory may then be directly compared to experiment and we may further test the inverse procedure. Here, we note only that the measured intensity distribution gives results that are of the correct order of magnitude. For example, the mean free path of scattering, l_F, may be defined for this experiment as $l_F = (\mu^2 k^2 \Lambda)^{-1}$. For strong scattering, we find l_F is approximately 6 m. (In the experiment $k = 4000\ m^{-1}$). The propagation path was 2.33 m so that we expect that roughly 30% of the beam was scattered. In addition, the transverse scattered distance at 2.33 m was $(2.33)/(k\Lambda)$, which is approximately 6 cm. These numbers, which are order of magnitude estimates, are consistent with the results of Table II.

Table II

Distance from beam axis (cm)	Intensity Weak Scattering (Normalized)	Intensity Strong Scattering (Normalized)
0	1.000	1.00
1	0.910	0.96
2	0.700	0.87
3	0.360	0.63
4	0.100	0.28
6	0.003+	0.034
8	0.011	0.032

+ near measurement system noise limit.

IX. Conclusions and Recommendations

The basic theory required for the development of a new acoustic technique for studying fine-to-intermediate scale processes and distributions of properties in the ocean have been successfully addressed. Insofar as we were able to test that theory, experiment and theory are in agreement. A critical need exists to understand ocean processes on scales of 100's of meters to centimeters. The tools and techniques that are currently available are inadequate. There are potential applications of such a tool in addressing key problems in underwater acoustics, and in physical, chemical and biological oceanography. We conclude, based on our results to date, that additional work is justified in pursuing this approach to a better description and understanding of intermediate-to-fine scale oceanography.

APPENDIX A

Effect of Random Velocity Fluctuations on Underwater Scattering

by

Mark J. Beran
and
Alan M. Whitman

School of Engineering
Tel Aviv University

Abstract

There is a well-developed theory to account for the effect of random fluctuations in the sound-speed on the underwater scattering of acoustic radiation. Here we show how the theory may be extended to include the effect of random fluctuations in fluid velocity. We assume that the characteristic time and length scales associated with the velocity correlation functions are long when compared to the corresponding scales (period and wavelength) of the acoustic radiation. We conclude with a discussion of the application of the theory to ocean studies and the utility of using an inverse method to find the lateral correlation function.

Introduction

In two recent articles[1,2], parabolic equations were derived to take into account the effect of ocean currents on sound transmission. Attention, in these papers, was limited to the effect of horizontal ocean currents. However, their formulation is easily extended to include a full three-dimensional velocity vector field, $\mathbf{v}(\mathbf{x})$. Here we are interested in the equations governing the coherence functions of the acoustic radiation and shall restrict our attention to random velocity fields that satisfy the following conditions:

a) $|\mathbf{v}|/c_o << 1$

b) $\omega T_c >> 1$

c) $kL_c >> 1$

where c_o is a characteristic speed of sound, ω is the radian frequency of the acoustic wave, k is the radiation wavenumber, T_c is the shortest characteristic time associated

with the velocity correlation functions and L_c is the smallest characteristic length associated with the velocity correlation functions.

With the above restrictions, it is possible to show that for a cw signal the spatial part of the pressure, $p(\mathbf{x})$, satisfies the equation

$$\nabla^2 p + k^2 p(\mathbf{x}) + 2ik_o \mathbf{v}(\mathbf{x}) \cdot \nabla p(\mathbf{x})/c = 0. \qquad (1)$$

In the derivation of Eq. (1) we used the conditions (a)-(c). It was not necessary to assume that the magnitude of the vertical component of the velocity was much smaller than that of the horizontal components.

To derive a parabolic equation we write

$$p(x,y,z) = u(x,y,z) \exp(ik_o z),$$

where z is the mean propagation direction, y the depth direction, x the cross-range direction and $k_o = \omega/c_o$. The first two terms of Eq. (1) yield the usual parabolic equation. The last term gives

$$2ik_o[\mathbf{v}_T \cdot \nabla_T p + v_z \partial u/\partial z \, (\exp(ikz)) + ik_o v_z p]/c_o.$$

In the appendix, we show that only the last term contributes to dominant order in the parabolic equation. We thus find

$$2ik_o \partial u/\partial z + \nabla_T^2 u + [k^2 - k_o^2 - 2k_o^2 v_z/c_o]u = 0. \qquad (2)$$

When the sound-speed fluctuations are small we may write

$$k^2 - k_o^2 = k_o^2[2(c - c_o)/c_o + 2c'/c_o],$$

where c is the mean speed of sound. This yields

$$2ik_o \partial u/\partial z + \nabla_T^2 u + k_o^2[\bar{\mu}(x) + \mu'(x)]u = 0 \qquad (3)$$

where $\bar{\mu}(x) = 2(c - c_o)/c_o$ and $\mu'(x) = 2(c' - v_z)/c_o$.

Eq. (3) is exactly the same equation as that used in studies of scattering of acoustic energy by sound-speed fluctations alone. The only difference is that here the velocity component in the range direction, v_z, has been added to c'. Therefore the entire statistical theory used to study scattering from sound-speed fluctuations alone may also be used when we wish to consider the effect of a random velocity field. In the next section we shall briefly review the relevant statistical equations and in the final section we shall discuss the application of the theory to real ocean studies.

Statistical Theory

To treat the problem of scattering from a stochastic point of view, we define the following coherence functions

$$\{\Gamma(\mathbf{x}_{T1},\mathbf{x}_{T2},z)\} = \{u(\mathbf{x}_{T1},z)u^*(\mathbf{x}_{T2},z)\} \tag{4}$$

$$\{L^1(\mathbf{x}_{T1},\mathbf{x}_{T2},\mathbf{x}_{T3},\mathbf{x}_{T4},z)\} = \{u(\mathbf{x}_{T1},z)u^*(\mathbf{x}_{T2},z)u^*(\mathbf{x}_{T3},z)u(\mathbf{x}_{T4},z)\}. \tag{5}$$

Here u^* denotes the complex conjugate of u and the vector $\mathbf{x}_T$ has the transverse coordinates x,y. The brackets, { }, denote an ensemble average.

The intensity, $\{I(\mathbf{x}_T,z)\}$, is found from $\{\Gamma(\mathbf{x}_{T1},\mathbf{x}_{T2},z)\}$ by setting $\mathbf{x}_{T1} = \mathbf{x}_{T2}$. The intensity fluctuations, $\{I^2(\mathbf{x}_T,z)\}$, and the coherence of intensities, $\{R_I(\mathbf{x}_{T1},\mathbf{x}_{T2},z)\}$, are found from $\{L^1\}$ from the following relations

$$\{I^2(\mathbf{x}_T,z)\} = \{L^1(\mathbf{x}_T,\mathbf{x}_T,\mathbf{x}_T,\mathbf{x}_T,z) \tag{6}$$

$$\{R_I(\mathbf{x}_{T1},\mathbf{x}_{T2},z)\} = \{L^1(\mathbf{x}_{T1},\mathbf{x}_{T1},\mathbf{x}_{T2},\mathbf{x}_{T2},z)\}. \tag{7}$$

We write $\mu(x)$ in the form

$$\mu(x) = \bar{\mu}(x) + \mu'(x), \tag{8}$$

where $\bar{\mu}(x)$ represents the mean background profile and $\mu'(x)$ represents the random fluctuation field. We shall assume here that the statistics of the field are homogeneous. The two-point correlation function, $\sigma(\mathbf{x}_1,\mathbf{x}_2)$, is defined as

$$\sigma(\mathbf{x}_1,\mathbf{x}_2) = \{\mu'(\mathbf{x}_1)\mu'(\mathbf{x}_2)\} \tag{9}$$

and depends upon $\mathbf{r} = \mathbf{x}_1 - \mathbf{x}_2$. In addition we define the function

$$\bar{\sigma}(\mathbf{x}_{T1} - \mathbf{x}_{T2}) = (1/4)\int_{-\infty}^{\infty} \sigma(\mathbf{x}_{T1} - \mathbf{x}_{T2},r_z)dr_z \tag{10}$$

The equations governing $\{\Gamma\}$ and $\{L^1\}$ (See Refs. 3 - 7) are

$$\partial\{\Gamma\}/\partial z = (i/2k_o)[\nabla^2_{T1} - \nabla^2_{T2}]\{\Gamma\} -$$

$$k_o^2[\bar{\sigma}(0) - \bar{\sigma}(\mathbf{x}_{T1} - \mathbf{x}_{T2})]\{\Gamma\} + ik_o[\bar{\mu}(\mathbf{x}_{T1}) - \bar{\mu}(\mathbf{x}_{T2})]\{\Gamma\} \tag{11}$$

$$\partial\{L^1\}/\partial z = (i/2k_o)[\nabla^2_{T1} - \nabla^2_{T2} - \nabla^2_{T3} + \nabla^2_{T4}]\{L^1\} +$$

$$k_o^2[\bar{\sigma}(\mathbf{x}_{T1} - \mathbf{x}_{T2}) + \bar{\sigma}(\mathbf{x}_{T1} - \mathbf{x}_{T3}) +$$

$$\bar{\sigma}(\mathbf{x}_{T2} - \mathbf{x}_{T4}) + \bar{\sigma}(\mathbf{x}_{T3} - \mathbf{x}_{T4}) -$$

$$\bar{\sigma}(\mathbf{x}_{T1} - \mathbf{x}_{T4}) - \bar{\sigma}(\mathbf{x}_{T2} - \mathbf{x}_{T3}) -$$

$$2\bar{\sigma}(0)]\{L^1\} + ik_o[\bar{\mu}(\mathbf{x}_{T1}) -$$

$$\bar{\mu}(\mathbf{x}_{T2}) - \bar{\mu}(\mathbf{x}_{T3}) + \bar{\mu}(\mathbf{x}_{T4})]\{L^1\} \qquad (12)$$

In the literature, there are many solutions of Eqs. (11) and (12) under a variety of conditions (see, for example, Refs. 3 - 18). It is not our purpose to review these solutions here, but rather to emphasize that any solution now available can be used to include the effects of random velocity fluctuations provided that the correlation function $\sigma(\mathbf{x}_1,\mathbf{x}_2)$ is defined as

$$\sigma(\mathbf{x}_1,\mathbf{x}_2) = 4\{[c'(\mathbf{x}_1) - v_z(\mathbf{x}_1)][c'(\mathbf{x}_2) - v_z(\mathbf{x}_2)]\}/c_o^2, \qquad (13)$$

rather than

$$\sigma(\mathbf{x}_1,\mathbf{x}_2) = 4\{[c'(\mathbf{x}_1)\,][c'(\mathbf{x}_2)]\}/c_o^2. \qquad (14)$$

In the next section, we discuss the ocean conditions under which we expect the random velocity fluctuations to have a significant effect when compared to the sound-speed fluctuations. We also shall briefly survey the measurements that are now available. Finally, we shall point out that if an inverse procedure is used to determine the lateral correlation function, σ , then for many problems it is not necessary to distinguish between the effects of sound-speed fluctuations and random velocity fluctuations.

Application to Ocean Problems

Much of the literature on ocean scattering of acoustic waves is devoted to scattering by internal waves. In this case, as Flatte[18] points out, the sound-speed fluctuations are of the order of a meter/sec while the fluid velocities are of the order of centimeters/sec. Thus the velocity fluctuations may safely be neglected.

If one is interested in the scattering of high frequency acoustic radiation, say 20-100 kHz, then the internal waves are generally no longer of paramount interest. Rather, one considers scales of the order of say,10 cm to 10 m. In this case the sound-speed fluctuations are of the order of perhaps 10 cm/sec or less, while the fluid velocities remain of the order of centimeters/sec. Hence we must consider the velocity fluctuations in scattering experiments, especially if we are interested in the effect of the 10-cm scale range. The variability of the ocean environment is so great and the measurements so sparse that it is dificult at this stage to give more than rough orders of magnitude for the fluid velocity fluctuations. We obtained the above figures from a survey of Refs. 19-24.

Knowledge of the speed of sound fluctuations in the 10 cm to 10 m range is greater than our knowledge of the velocity fluctuations (see, for example, Refs. 25-26), but still is hardly satisfactory. At the present time, we really do not have sufficient data to make good predictions of the intensity and intensity fluctuations, using Eqs.(11) and (12), even if we assume that sound-speed fluctuations are the dominant effect. Requiring an independent knowledge of velocity fluctuations is probably beyond our present measurement capabilities.

The problem of finding σ , when velocity fluctuations are present, is further complicated by the fact that Eq. (13) shows us that we must not only know the statistics of the velocity field itself, but must also know the function

$$\{c'(\mathbf{x}_1)v_z(\mathbf{x}_2)\}.$$

That is, we must know the correlation btween the sound-speed fluctuations and the horizontal range component of the velocity field. At present, we have virtually no knowledge of this function. However, if the sound-speed fluctuations and the velocity fluctuations are weakly correlated and this function can be set equal to zero, then the situation is much better. In that case the velocity fluctuation effect is of order $(v_z/c')^2$ and even if $O(v_z/c') = 1/3$, we can neglect the effect of velocity fluctuations.

Finally, we should like to point out that there is a method for determining $\bar{\sigma}$ which is independent of the relationship between c' and v_z. This is the inverse method for determining $\bar{\sigma}$ proposed in Ref. 10. The basic idea is to measure the intensity distribution or coherence function from a known acoustic source and then to invert the solution to find $\bar{\sigma}$. For example, the solution for the coherence function for a point source, in the absence of a background profile, is

$$\{\Gamma(\mathbf{s},z)\} = (I_z/z^2)\exp(-k^2z[\bar{\sigma}(0) - \int_0^1 \bar{\sigma}(a\mathbf{s})da]). \quad (15)$$

Here I_z is a normalization constant and $\mathbf{s} = \mathbf{x}_1 - \mathbf{x}_2$.

Eq. (15) may be inverted to find $\bar{\sigma}$. The inversion formula is

$$\bar{\sigma}(s_x) = \bar{\sigma}(0) + d/ds_x[(s_x/k^2z)\log(\{\Gamma(s_x,z)\}/(I_z/z^2))], \quad (16)$$

with $s_y = 0$. There is a similar expression for s_y when $s_x = 0$.

This method was used by Coles and Frehlich[28] to measure $\bar{\sigma}$ for light propagation in the turbulent atmosphere. We have less experience measuring the coherence function in the ocean, but it appears to be possible. If the coherence measurement is impractical, however, we may use instead a directed Gaussian beam as a source. In this later case, only the intensity need be measured in order to be able to invert the solution to find $\bar{\sigma}$.[10]

Summary

In this paper we have shown how to take into account the effect of a random fluid velocity field on the scattering of acoustic radiation in the ocean. The analysis is subject to the restrictions (a)-(c) given in the Introduction. It is then pointed out that in high frequency scattering, where scales of the order of meters become important, it may be necessary to consider the effect of velocity fluctuations. Finally, the inverse procedure of determining $\bar{\sigma}$ is discussed. This method does not require independent measurements of sound-speed and fluid velocity fluctuations.

References

1. J. S. Robertson, W. L. Siegman and M. J. Jacobson, "Current and current shear effects in the parabolic approximation for underwater sound channels," J. Acoust. Soc. Amer. 77, 1768-1780 (1985).

2. L. Nghiem-Phu and F. Tappert, "Parabolic equation modeling of the effects of ocean currents on sound transmission and reciprocity in the time domain," J. Acoust. Soc. Amer. 78, 642-648 (1985).

3. V. I. Shishov, "Theory of wave propagation in random media," IVUZ-Radiophysics (Russian).11, 866 (1968).

4. M.J. Beran and T. L. Ho " Propagation of the fourth-order coherence function in a random medium (a nonperturbative formulation)", J. Opt. Soc. Amer. 59, 1134 (1969).

5. V. I. Tatarski: The Effects of The Turbulent Atmosphereon Wave Propagation, translated from the Russian and available from the National Technical Information Service (Springfield, Virginia 1971).

6. B. J. Uscinski: The Elements of Wave Propagation in Random Media, (McGraw Hill, New York, 1977).

7. A. Ishimaru: Wave Propagation and Scattering in Random Media, Vols. 1 and 2 (Academic Press, New York 1978).

8. B. J. Uscinski " Intensity fluctuations in a multiple scattering medium. Solution of the fourth moment equation", Proc. Roy. Soc. Lond. A380, 137 (1982).

9. C. Macaskill " An improved solution to the fourth moment equation for intensity fluctuations," Proc. Roy. Soc. Lond. A386, 461 (1983).

10. S. Frankenthal, A. M. Whitman and M. J. Beran: "Two-scale solutions for intensity fluctuations in strong scattering", J. Opt. Soc. Amer. 1, 585 (1984).

11. A. M. Whitman and M. J. Beran: "Two scale solution for atmospheric scintillation," J. Opt. Soc. Amer. A2, 2133-2143 (1985).

11a. M. J. Beran: "The inverse problem in a random medium", SPIE, Proc. Inverse Optics", 413, 61 (1983).

11b. A. M. Whitman and M. J. Beran: "Beam spread of laser light propagating in a random medium", J. Opt. Soc. Amer. 60, 1595 (1970).

12. M. J. Beran and J. J. McCoy: " Propagation through an anisotropic random medium", J. Math. Phys. 15, 1901-1912 (1974).

13. M. J. Beran, J. J. McCoy: " Propagation of radiation from a finite beam or source through an anisotropic random medium", J. Acoust. Soc. Am. 56, 1667-1672 (1974).

14. M. J. Beran, J. J. McCoy: "Propagation through an anisotropic random medium. An integro-differential formulation", J. Math. Phys. 17, 1186-1189 (1976).

15. M. J. Beran, J. J. McCoy: " A cylindrically symmetric coherence formulation for the ocean", J. Acoust. Soc. Amer. 61, 596-599 (1977).

16. M. J. Beran and A. M. Whitman: "Scattering of a finite beam in a random medium with a nonhomogeneous background", . Math. Phys. 16, 214-217 (1975).

17. M. J. Beran, A. M. Whitman and S. Frankenthal: "Scattering calculations using the characteristic rays of the coherence function", J. Acoust. Soc. Amer. 71, 1124-1130 (1982).

18. S. M. Flatte, R. Dashen, W. H. Munk, K. M. Watson, F. Zachariasen: Sound Transmission Through a Fluctuating Ocean (Cambridge University Press, Cambridge, 1979).

19. H. L. Grant, R. W. Stewart and A. Moilliet: "Turbulent spectra from a tidal channel", J. Fluid Mech. 12, 241-268 (1962).

20. T. R. Osborn: " Vertical profiling of velocity microstructure", J. Phys. Ocean., 4 109-115 (1974).

21. A. E. Gargett: "An investigation of the occurence of oceanic turbulence with respect to finestructure", J. Phys. Ocean. 6, 139-156 (1975).

22. N. S. Oakey: "Determination of the rate of dissipation of turbulent energy for simultaneous temperature and velocity shear microstructure measurements", J. Phys. Ocean., 12 256-271 (1983).

23. M. D. Levine, C. A. Paulson and J. M. Morison: "Internal waves in the Arctic: Comparison with lower-latitude observations", J. Phys. Ocean., 15 800-809 (1985).

24. T. R. Osborn and R. G. Lueck: "Turbulent measurements with a submarine", J. Phys. Ocean., 15 1502-1520 (1985).

25. R. F. Shvachko: "Sound fluctuations in the upper layer of the ocean and their relation to random inhomogeneities of the medium", Sov. Phys. - Acoust., 9 280-282 (1964).

26. R. F. Shvachko: "Sound fluctuations and random inhomogeneities in the ocean", Sov. Phys. - Acoust., 13 93-97 (1967).

27. R. Garrison and T. Wen: "High frequency acoustic variability in the arctic", J. Acoust. Soc. Amer., 77 465-481 (1985).

28. W. A. Coles and R. G. Frehlich: "Simultaneous measurements of angular scattering and intensity scintillation in the atmosphere", J. Opt. Soc. Amer., 72 1042 (1982).

Appendix

We write Eq. (1) in dimensionless form using l_z as a characteristic range coordinate and l_T as a characteristic transverse coordinate. We denote U as a characteristic velocity. We then have

$$(1/(kl_z)^2)\,\partial^2 p/\partial z^2 + (1/(kl_T)^2)\,\nabla_T^2 p + n^2 p + 2iM(1/(kl_z))n^2 v_z\,\partial p/\partial z + 2iM(1/(kl_T))n^2 \mathbf{v}_T \cdot \nabla_T p = 0, \quad \text{(A1)}$$

where $n = c_o/c$, $M = U/c_o$ and the independent variables appearing here are dimensionlized by l_T and l_z.

Under the transformation

$$p = u \exp(ikl_z z)$$

Eq. (A1) becomes

$$(n^2 - 1)u - 2Mv_z n^2 u + 2i(1/kl_z)\,\partial u/\partial z + (1/(kl_z)^2)\,\partial^2 u/\partial z^2 + (1/(kl_T)^2)\nabla_T^2 u + 2iM(1/kl_z)n^2 v_z\,\partial u/\partial z - 2iM(1/kl_T)n^2 \mathbf{v}_T \cdot \nabla_T u = 0. \quad \text{(A2)}$$

In the limit $kl_z >> 1$, the term $(1/(kl_z)^2)\,\partial^2 u/\partial z^2$ may be neglected and Eq. (A2) is parabolic. However, in order that Eq. (A2) include the effects of index of refraction variations and diffraction, we assume that that other terms are of the same order as $(1/kl_z)\,\partial u/\partial z$. Thus, for example, the longitudinal and transverse scales are related by the equality

$$kl_z = (kl_T)^2 \quad \text{(A3)}$$

or $l_z = kl_T^2$. Furthermore, we demand that the term $(n^2 - 1)u$ is of the same order as the term $2i(1/kl_z)\,\partial u/\partial z$. Then, if we write

$$(n^2 - 1) = 2(c - c_o)/c_o = 2n' = \langle n'^2 \rangle^{1/2} f(x), \quad \text{(A4)}$$

where $\langle n'^2 \rangle^{1/2}$ is a measure of the size of the variations in n', we have

$$\langle n'^2 \rangle^{1/2} = 1/kl_z. \quad \text{(A5)}$$

Eq. (A5) represents a choice for l_z. It also represents a restriction on the size of $\langle n'^2\rangle^{1/2}$ since we have already required that $1/kl_z << 1$. This is the restriction to weak scattering. In addition, since now $l_T/l_z = \langle n'^2\rangle^{1/4}$, we have the restriction to forward scattering.

Here, we also require that $M << 1$ and that $M = m\langle n'^2\rangle^{1/2}$, where $m = O(1)$. With this scaling, the last two terms in Eq. (A2) may be neglected. We find, finally,

$$2i\,\partial u/\partial z + \nabla_T^2 u + 2(n' - Mv_z) = 0, \qquad \text{(A6)}$$

which leads to Eq. (2).

Finally, we note that the last term in Eq. (A2) is the largest term neglected when $m = O(1)$ and sets the limit on the validity of the approximations.

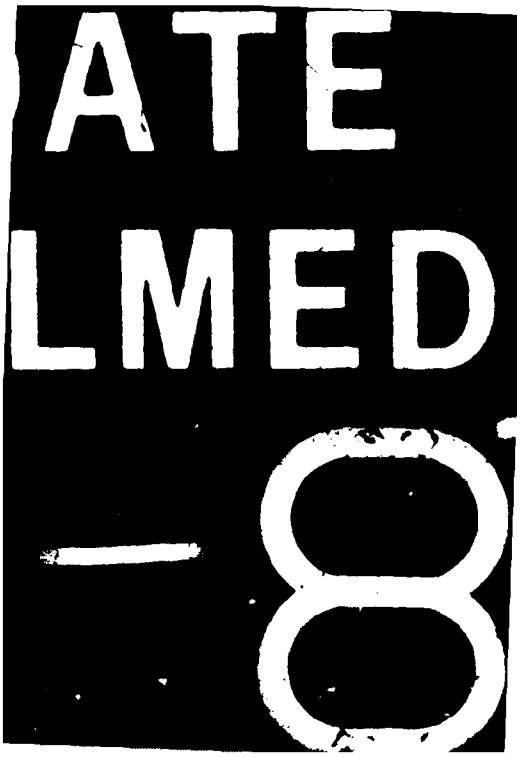
ATE
LMED
8